Cooling reverses pathological bifurcations to spontaneous firing caused by mild traumatic injury

B. M. Barlow, B. Joos, A. K. Trinh, and A. Longtin

Citation: Chaos **28**, 106328 (2018); doi: 10.1063/1.5040288
View online: https://doi.org/10.1063/1.5040288
View Table of Contents: http://aip.scitation.org/toc/cha/28/10
Published by the American Institute of Physics

Articles you may be interested in

Neuron dynamics variability and anomalous phase synchronization of neural networks
Chaos: An Interdisciplinary Journal of Nonlinear Science **28**, 106304 (2018); 10.1063/1.5023878

Existence and stability of chimera states in a minimal system of phase oscillators
Chaos: An Interdisciplinary Journal of Nonlinear Science **28**, 103121 (2018); 10.1063/1.5044750

Describing dynamics of driven multistable oscillators with phase transfer curves
Chaos: An Interdisciplinary Journal of Nonlinear Science **28**, 106323 (2018); 10.1063/1.5037290

Two-dimensional spatiotemporal complexity in dual-delayed nonlinear feedback systems: Chimeras and dissipative solitons
Chaos: An Interdisciplinary Journal of Nonlinear Science **28**, 103106 (2018); 10.1063/1.5043391

Synchronous tonic-to-bursting transitions in a neuronal hub motif
Chaos: An Interdisciplinary Journal of Nonlinear Science **28**, 106315 (2018); 10.1063/1.5039880

Bottom-up approach to torus bifurcation in neuron models
Chaos: An Interdisciplinary Journal of Nonlinear Science **28**, 106317 (2018); 10.1063/1.5042078

Cooling reverses pathological bifurcations to spontaneous firing caused by mild traumatic injury

B. M. Barlow, B. Joos, A. K. Trinh, and A. Longtin
Department of Physics, Centre for Neural Dynamics, University of Ottawa, 150 Louis Pasteur Priv., Ottawa, Ontario K1N6N5, Canada

(Received 16 May 2018; accepted 23 August 2018; published online 25 October 2018)

Mild traumatic injury can modify the key sodium (Na^+) current underlying the excitability of neurons. It causes the activation and inactivation properties of this current to become shifted to more negative trans-membrane voltages. This so-called coupled left shift (CLS) leads to a chronic influx of Na^+ into the cell that eventually causes spontaneous or "ectopic" firing along the axon, even in the absence of stimuli. The bifurcations underlying this enhanced excitability have been worked out in full ionic models of this effect. Here, we present computational evidence that increased temperature T can exacerbate this pathological state. Conversely, and perhaps of clinical relevance, mild cooling is shown to move the naturally quiescent cell further away from the threshold of ectopic behavior. The origin of this stabilization-by-cooling effect is analyzed by knocking in and knocking out, one at a time, various processes thought to be T-dependent. The T-dependence of the Na^+ current, quantified by its $Q_{10\text{-}Na}$ factor, has the biggest impact on the threshold, followed by $Q_{10\text{-}pump}$ of the sodium-potassium exchanger. Below the ectopic boundary, the steady state for the gating variables and the resting potential are not modified by temperature, since our model separately tallies the Na^+ and K^+ ions including their separate leaks through the pump. When only the gating kinetics are considered, cooling is detrimental, but in the full T-dependent model, it is beneficial because the other processes dominate. Cooling decreases the pump's activity, and since the pump hyperpolarizes, less hyperpolarization should lead to more excitability and ectopic behavior. But actually the opposite happens in the full model because decreased pump activity leads to smaller gradients of Na^+ and K^+, which in turn decreases the driving force of the Na^+ current. *Published by AIP Publishing.*
https://doi.org/10.1063/1.5040288

Experimental studies have revealed that mild trauma in the form of, e.g., physical pressure or chemical stimuli can alter the properties of the main current (sodium) responsible for the voltage swings or "firings" of neurons. This leads to ongoing firings even when the cell should be quiescent. Such pathological firing interferes with the usual input integration properties of the cell, and in particular has been implicated in the genesis of pathological pain, which persists even after the injury-producing stimulus is removed. From a dynamical point of view, this mild trauma lowers the threshold for firing. This paper explores the possibility of using temperature to offset this effect by raising the firing threshold back up. Our modeling study predicts that cooling the neuron by just a few degrees—as is possible, e.g., for peripheral nerve cells—can counteract the pathological state. The sensitivity of the sodium current to temperature is the key determinant of this effect.

I. INTRODUCTION

Temperature is an important determinant of excitable behavior since it has a direct effect on the kinetics of every chemical reaction. This includes the rates of transitions between open and closed states of ionic channel proteins, as well as ionic exchangers and channel conductances. In the central nervous system (CNS), the temperature is tightly controlled to enable normal cellular function. In the peripheral nervous system, and especially in nerves near the skin surface, the temperature can vary over a greater range, according to the external temperature, and the excitability is adapted to accommodate a range of functions. In fact, specialized neurons known as thermoreceptors in the skin and elsewhere continually report a wide range of local temperatures to the CNS.

Injury in the form of a mild stretching of nerve membrane has been shown to cause a concomitant shift in the voltage-dependence of the activation and inactivation gating characteristics of sodium channels.[1] This so-called "coupled left shift" or CLS causes the cell to become more "leaky," which means that the small Na current around the resting potential of the cell is now stronger.[2] When the left shift is sufficiently strong, it can lead to repetitive firing of action potentials (APs or "spikes" or "firings") originating in the damaged section of the axon. This section then produces APs when it normally should not, i.e., it exhibits "ectopic" firing. The job of the axon is to propagate action potentials that arose at the axon initial segment just outside the soma down to target neurons, not to produce its own APs. Target cells are then continually receiving currents at their synapses from such pathologically firing cells. CLS can also affect the soma directly and interfere with its integration properties.

CLS has been modeled mathematically by a simple addition of a left shift (LS) to the voltage of the activation (m) and inactivation (h) gates for the sodium current in the standard Hodgkin-Huxley (HH) formalism.[2,3] Under fairly

generic conditions, as *LS* increases, a bifurcation first occurs from quiescence to a bursting firing pattern in which APs are arranged in clusters separated by quiescent phases. The bursting involves a rapidly firing phase, followed by a quiescent phase, and the whole pattern repeats. As *LS* increases even more, another bifurcation occurs, this time from bursting to tonic firing. At this transition, the quiescent interval between the clusters of spikes has shrunk such that only the rapidly firing "tonic" phase remains. These bifurcations are summarized in Fig. 1 for the more detailed HH model we present below. It is in fact a phase diagram illustrating the position of the tonic and bursting solutions in the two-dimensional subspace spanned by the *LS* parameter and the *AC* parameter that quantifies the fraction of channels affected by CLS.

A dynamical analysis of these solutions and their bifurcations at a single node of Ranvier was reported in Ref. 4. There, a numerical bifurcation tool was used as well as a slow-fast analysis: the fast sub-system generates the rapid limit cycle associated with the spikes during the active phase of the burst, while the dynamics of the Nernst potentials form the slow one (see Sec. II). In the context of transmission down an axon, CLS has negative consequences on information transmission, especially at low frequencies.[5] Bursting is also associated with the presence of subthreshold oscillations, which have been implicated in neuropathic pain, i.e., pain signals that outlast the injury.[6–8] In fact, it appears that the joint effect of such oscillations and noise, associated with channel conductance fluctuations and other sources of cellular stochasticity, produces firing patterns that highly resemble those seen in the context of neuropathic pain.

These "injured" ectopic dynamics set the stage for investigating the role played by temperature in injured cells. Temperature (T) is part of the original HH formalism,[3] which includes a temperature factor in the equations for the three gating variables: m and h for the voltage-gated Na^+ channel (or Nav), and n for the voltage-gated K^+ channel (or Kv) (see below). But the effect of temperature extends beyond simply speeding up kinetics. It is generally assumed that increases in temperature also lead to higher conductances and to stronger ionic pump activity.[9]

If T is too high, the standard HH axon loses its ability to generate APs altogether, i.e., it undergoes conduction block (see Ref. 10 for a more recent survey). In therapeutic applications, it is also known that the ability of a neuron to respond to high frequency biphasic stimulation is temperature dependent.[11] Beyond a certain threshold frequency, the nerve conduction is blocked, but this threshold increases with temperature. At some point, the smaller refractory period at higher T loses to inactivation and repolarizing forces. But before this point is reached, T changes can significantly alter firing patterns. In the majority of cells in the CNS, this is bad news, but for non-noxious thermoreceptors in the periphery as well as in specialized areas of the CNS (hypothalamus), the variation in firing pattern encodes the information about T changes, and the body can adapt by, e.g., sweating to remove heat or shivering to generate heat.

It has been shown that, upon cooling a nerve, its axons conduct more slowly. Given that there is already a distribution of propagation velocities due to heterogeneity in axon diameters, the cooling will cause a bigger "dispersion" in time delays of propagation down the nerve, as predicted in model studies.[12] One consequence of this enhanced temporal dispersion is thought to be the loss of synchrony of activation of postsynaptic targets, with possible clinical manifestations.

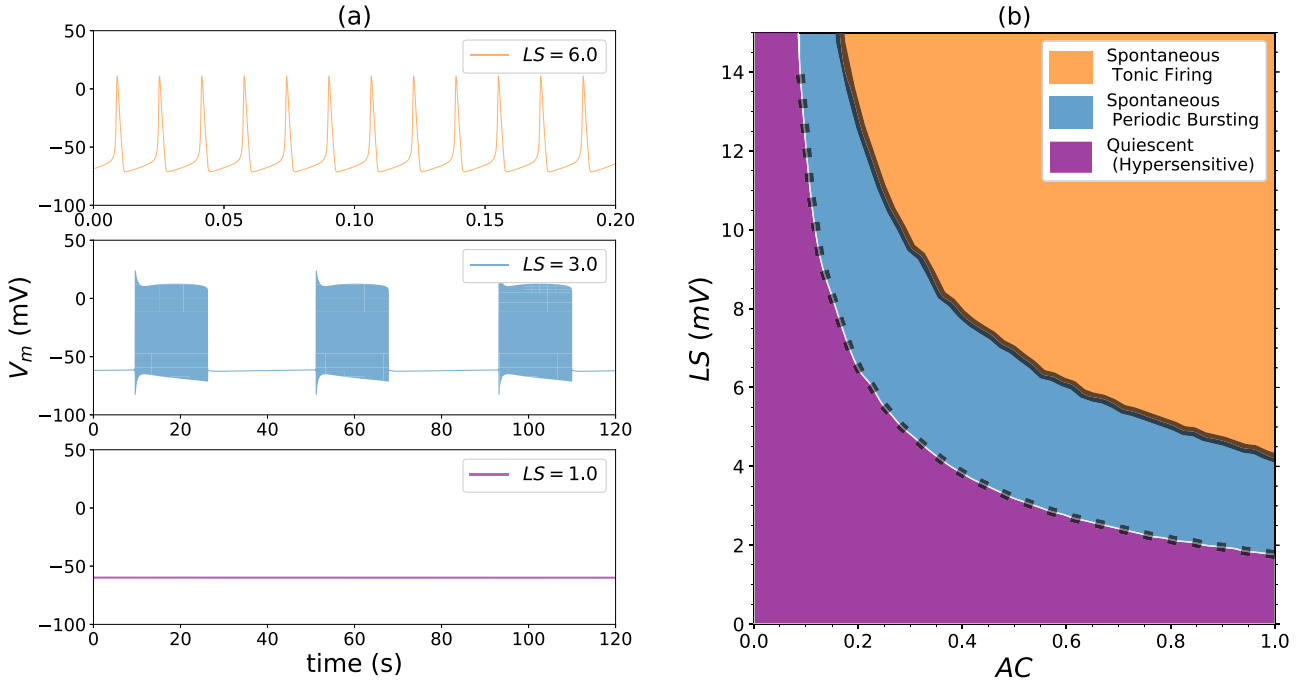

FIG. 1. As the left-shift (*LS*) voltage increases, the system becomes ectopic. In (a), time series of the membrane potential are shown with all channels left-shifted by the amount indicated; in other words, the fraction of affected channels (*AC*) equals 1. Damage increases from the bottom plot upward. The regime diagram (b) features two boundaries. The lower boundary (dashed black line) is the bursting threshold. Below it, the node remains stable (quiescent regime). Above this threshold, the node becomes ectopic: at first bursting spontaneously and then firing tonically above the upper boundary.

Increased T is known to favor conduction block in central demyelinated axons,[13] which is one of the explanations for the worsening of symptoms of multiple sclerosis upon warming (and improvement upon cooling—see Ref. 14 for a review of the early literature on this topic). Actually, nerve conduction studies use temperature as a parameter to help disambiguate problems relating to conduction block from those related to changes in dispersion.[10] Mild cooling of the brain, e.g., by 3° to 4°, is also used as a neuroprotective measure following, e.g., stroke and traumatic brain injury as it reduces metabolism, fever, excitotoxicity (overactivation of glutamate receptors), and intracranial pressure.[15] Another recent study[16] of the effect of temperature on excitability parameters in human motor axons reveals predictable effects such as increased refractory period upon cooling. But other effects, especially on sensory axons, were more ambiguous, and complicated by the transient nature of certain currents such as the transient hyperpolarization induced by warming; the latter increases the activity of the Na^+/K^+ electrogenic pump, the net effect of which is one positive charge pushed out of the cell on each cycle (included in our model below).

In this paper, we address the following question: given that mild injury can cause a transition from quiescence to pathological firing and that temperature modulates excitability, is there a way for changes in temperature to reverse the negative effects of CLS, at least in a qualitative sense? Our model below lays the groundwork to formulate this question biophysically, computationally, and from a nonlinear dynamics perspective and provides some answers. Our model of T- and CLS-dependent ectopy, or T-CLS for short, is inspired by cold receptor models. Such neurons are tasked with reporting the static and time-dependent changes in ambient temperature at various places on the body, mainly on the skin including the eyes and tongue. They are free nerve endings that branch out from a myelinated axon whose soma lies in the dorsal root ganglion in the spinal cord. Cold receptors increase their firing rate upon cooling; warm receptors do the opposite, and although they are well-documented, their dynamics have not yet been modeled. Cold thermoreceptors actually work using a noisy subthreshold oscillation, the amplitude and frequency of which are T-dependent. This has been described experimentally[17–19] as well as in computational models.[20,21] The patterns of activity of cold receptors range from bursting to tonic (i.e., periodic without spike clustering), and then to a form of tonic firing where spikes appear randomly deleted from a periodic sequence. These were documented early on by Braun, Hensel, and Schäfer and their colleagues in Marburg.[18,19]

Our model formulation thus takes advantage of the knowledge gained from decades of study of temperature-induced firing pattern changes in thermoreceptors. The paper is organized as follows. In Sec. II, we recall the CLS model and discuss how to implement temperature-sensitivity. Results that address the question raised above are then presented, first on CLS and then on T-CLS, culminating in a phase diagram that involves only T and LS. We go on to dissect the various components of this temperature correction to the CLS effects. The paper ends with a Discussion and outlook onto future questions.

II. MODEL

A. The Coupled Left Shift (CLS) model of nodal damage

The model presented here has been used previously to describe the dynamics of the trans-membrane voltage at a single node of Ranvier in a myelinated axon.[2,4] Such nodes, about a micron in length, are about a millimeter apart along the length of the axon. We focus strictly on the behavior of one node; CLS-induced disruptions to propagating action potentials and information processing have been recently discussed,[5] and the T-dependent properties of these effects are beyond the scope of our study. Axonal voltage excursions were modeled at an individual node of Ranvier with the Hodgkin-Huxley (HH) model using the values in Ref. 2 (and similar to those in Refs. 4, 5, and 22). The parameter values and meaning are listed in Table I. We start with the basic equation for the membrane potential (V_m written as V for simplicity),

$$C\frac{dV}{dt} = -I_{Na} - I_K - I_{pump} - I_{Naleak} - I_{Kleak} - I_{leak}, \quad (1)$$

where C is the specific nodal membrane capacitance. The total current density I_{Na} through the Nav channels is $I_{Na} = g_{Na}(V - E_{Na})$, where $g_{Na} = \bar{g}_{Na}m^3h$ (m and h are gating variables, the former measuring the activation and the latter the inactivation, but is also known as the availability). Likewise, the total current density I_K through Kv channels is $I_K = g_K(V - E_K)$, with $g_K = \bar{g}_K n^4$. Here, $\bar{g}_{Na}$ and $\bar{g}_K$ are the maximal conductances of the Nav and Kv channels, respectively; E_{Na} and E_K are the sodium and potassium Nernst

TABLE I. Parameters for the node of Ranvier model with temperature dependence

Membrane capacitance	$C = 1\ \mu F/cm^2$
Maximal Nav conductance	$\bar{g}_{Na} = 120\ mS/cm^2$
Maximal Kv conductance	$\bar{g}_K = 36\ mS/cm^2$
Faraday constant	$F = 96\,485.3399$ C/mol
Constant	$R = 8.314\,459\,8$ CV/(mol K)
Temperature	$T_0 = 293.15$ K
Volume of inside compartment	$Vol_i = 3\ \mu m^3$
Volume of outside compartment	$Vol_o = 3\ \mu m^3$
Surface area of node	$A = 6 \times 10^{-8} cm^2$
Initial inside Na^+ concentration	$[Na^+]_i = 20$ mM
Initial outside Na^+ concentration	$[Na^+]_o = 154$ mM
Initial inside K^+ concentration	$[K^+]_i = 150$ mM
Initial outside K^+ concentration	$[K^+]_o = 6$ mM
Initial Na^+ Nernst potential	$E_{Na} = 51.5$ mV
Initial K^+ Nernst potential	$E_K = -81.3$ mV
Pump K^+ leak conductance	$g_{Kleak} = 0.1\ mS/cm^2$
Pump Na^+ leak conductance	$g_{Naleak} = 0.25\ mS/cm^2$
Leak conductance	$g_{leak} = 0.5\ mS/cm^2$
Leak reversal potential	$E_{leak} = -59.9$ mV
Maximum pump current	$I_{maxpump} = 90.9\ \mu A/cm^2$
Pump K^+-dissociation constant	$K_{M_K} = 3.5$ mM
Pump Na^+-dissociation constant	$K_{M_{Na}} = 10$ mM
Q_{10} for the kinetic constants	$Q_{gate} = 3.0$
Q_{10} for the Nav conductance	$Q_{Na} = 1.4$
Q_{10} for the Kv conductance	$Q_K = 1.1$
Q_{10} for the Na^+/K^+ pump	$Q_{pump} = 1.9$

reversal potentials, respectively; and n^4 gives the open probability of potassium channels. In the HH formulation, gating variables m, h, and n evolve according to

$$\frac{dm}{dt} = \alpha_m(1-m) - \beta_m m, \tag{2}$$

$$\frac{dh}{dt} = \alpha_h(1-h) - \beta_h h, \tag{3}$$

$$\frac{dn}{dt} = \alpha_n(1-n) - \beta_n n. \tag{4}$$

The forward (α_m and α_h) and backward rate functions (β_m and β_h) describe the first-order transitions between activation (m) and inactivation (h) processes in Eqs. (4) and (5), and are functions of the membrane voltage V:

$$\alpha_m = 0.1\frac{(V+40)}{1-\exp[-(V+40)/10]}, \tag{5}$$

$$\beta_m = 4\exp[-(V+65)/18], \tag{6}$$

$$\alpha_h = 0.07\exp[-(V+65)/20], \tag{7}$$

$$\beta_h = \frac{1}{1+\exp[-(V+35)/10]}. \tag{8}$$

The rate functions α_n and β_n for the potassium gating variable n in Eq. (4) also depend on V as

$$\alpha_n = 0.01\frac{(V+55)}{1-\exp\left(-\frac{V+55}{10}\right)}, \tag{9}$$

$$\beta_n = 0.125\ \exp\left(-\frac{V+65}{80}\right). \tag{10}$$

Experimental findings for recombinant I_{Na} from nodal type Nav1.6 channels[1] show that mechanical injury causes an irreversible hyperpolarizing ("left")-shift to the sodium activation and inactivation variables. The steady-state product of activation and inactivation, $m^3h(V)_{t\to\infty}$, i.e., the window conductance, also left-shifts. This CLS can be modeled[2,4] by replacing in the dynamics of m and h the membrane voltage V by $(V+LS)$.

However, axon injury is spatially non-homogeneous[23] and is therefore likely to result in spatially inhomogeneous CLS. We do not consider this situation here: when an LS is applied, it is done so to all Nav channels homogeneously.

To discuss issues related to ectopic firing, we have to keep track of the movements of the two ions involved in excitability and introduce Na^+/K^+ ATPase pumps. It is a reasonable assumption that the net flows of Na^+ and K^+ are zero when averaged over time and the cell is in its "healthy" excitable state. There are many cellular components that take part in maintaining homeostasis, and the precise way in which all these components interact is complex and not fully understood. Our model cannot take into account all these factors. Thus, we only add the Na^+/K^+ pump and the Na^+ and K^+-specific leak currents. Note that the resulting formalism goes beyond the standard Goldman-Hodgkin-Katz (GHK) equations by explicitly including the main putative processes that sustain the ionic gradients.

Our strategy has been to set up the system in a homeostatic state for the healthy node to better address the consequences of the additional demand on the availability of ionic resources, especially with respect to the maintenance of the gradients, which determine the Nernst potentials. This required keeping track of the movement of the Na^+ and K^+ ions. This setup was used in our previous work[2,4,5] on which this current study is based. CLS is such an increased demand. When the CLS is small, the system equilibrates to a new quiescent state with reduced gradients, reflected in a shift in the Nernst potentials. As you increase CLS beyond a certain point, there is a transition in which the steady-state Na^+ current, known as "window current," is sufficient to trigger action potentials. In this case, there is a new steady state in which the Nernst potentials are time-varying.

The sodium-potassium exchanger or Na^+/K^+ pump produces a current

$$I_{pump} = I_{maxpump}\left(1+\frac{K_{M_K}}{[K^+]_o}\right)^{-2} \times \left(1+\frac{K_{M_{Na}}}{[Na^+]_i}\right)^{-3}, \tag{11}$$

where $I_{maxpump}$ is the maximal current generated by the pump, K_{M_K} and $K_{M_{Na}}$ are Michaelis-Menten kinetic constants, and the Na^+ and K^+ currents flowing through the pump are $I_{Napump} = 3I_{pump}$ and $I_{Kpump} = -2I_{pump}$ since the pump moves out 3 Na^+ ions while bringing in 2 K^+ ions every cycle (its net effect is thus to hyperpolarize the inside of the cell).

The pump continually works. Its rate is determined by the inner and outer ion concentrations $[Na^+]_i$ and $[K^+]_o$, and the Michaelis-Menten constants which give the values of those concentrations at which the capture rate of the pump for a given ion is at half maximum. However, these constants do not determine the equilibrium concentrations of the Na^+ and K^+ ions, rather these are determined by balancing the total charge [Eq. (1)] and the currents associated with the ionic species Na^+ and K^+.

Finally the model includes the following leak currents which are as usual given by

$$I_{Naleak} = g_{Naleak}(V-E_{Na}); \quad I_{Kleak} = g_{Kleak}(V-E_K);$$
$$I_{leak} = g_{leak}(V-E_{leak}). \tag{12}$$

The concentrations of Na^+ and K^+ inside and outside the cell are then governed by

$$\frac{d[Na^+]_i}{dt} = -\frac{(I_{Na}+I_{Napump}+I_{Naleak})A}{FVol_i}, \tag{13}$$

$$\frac{d[Na^+]_o}{dt} = \frac{(I_{Na}+I_{Napump}+I_{Naleak})A}{FVol_o}, \tag{14}$$

$$\frac{d[K^+]_i}{dt} = -\frac{(I_K+I_{Kpump}+I_{Kleak})A}{FVol_i}, \tag{15}$$

$$\frac{d[K^+]_o}{dt} = \frac{(I_K+I_{Kpump}+I_{Kleak})A}{FVol_o}, \tag{16}$$

where F is the Faraday constant, A is the area of the node, and Vol_i and Vol_o the inner and outer volumes of the node. We made the extracellular volume equal to the intracellular volume for simplicity. There is no qualitative change in behavior when the exterior volume is varied relative to the interior volume (see Fig. 11 in Ref. 2). Just as a note, the intracellular

volume was chosen as fairly small to observe phenomena over relatively short time scales.

Finally, the Nernst potentials for the Nav and Kv currents are given by

$$E_{Na} = -\frac{RT}{F} \ln \frac{[Na^+]_i}{[Na^+]_o}, \tag{17}$$

$$E_K = -\frac{RT}{F} ln \frac{[K^+]_i}{[K^+]_o}, \tag{18}$$

and they will vary if T changes, or following anything that changes the concentration ratios of each ion type. We recall that neuron excitability is based on low $[Na^+]_i$ and high $[Na^+]_o$ (or positive E_{Na}) working together with a high $[K^+]_i$ and low $[K^+]_o$ (or negative E_K).

A phase diagram for this model is shown in Fig. 1, along with examples of quiescent, bursting, and tonic firing patterns. Bursting does not occur in the standard four-dimensional HH system. Rather, an additional slow subsystem is required, which increases the dimensionality of the system. In our system, bursting arises due to the slow changes in ionic concentrations in Na^+ and K^+ ions, which in turn affect the Nernst potentials; these provide the battery power to generate action potentials in the first place.[2,4] Bursting is then a consequence of the fact that, during the active firing phase of the burst, the ionic gradients become depleted, and the Nernst potentials move toward zero (from above in the case of E_{Na} and from below in the case of E_K). Once they are too depleted, firing ceases, and homeostatic forces, namely the Na^+/K^+ pump, recharge the batteries until firing starts up again. In the healthy case, this depletion is kept in check by the pump; however, the increased leakiness caused by CLS is an extra load on the pump, and eventually it cannot keep up, and ectopic bursting ensues. At high LS values, a bifurcation from quiescence directly to tonic firing can occur.[24]

The bursting is organized around a subcritical Hopf bifurcation in the quiescent state. The slow dynamics move the state point past this bifurcation, and the solution is drawn to a stable fast spiking limit cycle. The Nernst potentials begin to deplete, and at some point, the solution falls off the fast limit cycle onto the lower fixed point branch of the subcritical Hopf point. The precise mechanism by which this drop to the quiescent phase occurs has not been worked out in full detail due to its complexity, as it occurs in the vicinity of a period-doubling cascade. In some cases, the last spikes in the burst reflect the presence of that cascade, and the bursting solutions appear to be chaotic rather than strictly periodic.[4] In any case, the presence of the Hopf produces decaying oscillations in voltage at the end of the burst phase, as well as at the end of the quiescent phase. This explains the relevance of this form of bursting with subthreshold oscillations to observations in the context of neuropathic pain.[2,4,6–8] Temperature effects reported below preserve these subthreshold oscillations, although a thorough bifurcation analysis is beyond the scope of our paper.

B. Incorporating temperature dependence

We wish to study the effect of temperature on the pathological behavior of the CLS model. Ideally, we would like to see how temperature plays off against, or along with, the LS factor. A lot of our knowledge about the effect of temperature on neurons comes from studies of cellular pacemakers. Willis *et al.*[25] as well as Wiederhold and Carpenter[26] have in fact advocated using pacemakers as model systems for thermoreceptors. Until recently, thermoreceptors were thought to do their work by virtue of the temperature-dependence of the basic processes underlying their excitability. In other words, there did not seem to be any "specialized" temperature receptor. The situation has changed for more than a decade now since TRP receptors were discovered. They are thought to underlie part of the cold and warm sensitivity, and especially the extreme warm sensitivities seen, e.g., in snakes and vampire bats. The TRP channel variety present in many cold receptors, TRPM8, has in fact been incorporated in a recent model for cold thermoreception.[27] This is a fascinating and rapidly moving field, which we will stay away from because we are considering the effect of temperature on generic nerve cells, not thermoreceptors with their specific complement of TRP channels.

Temperature is known to affect the ratio of the maximal sodium to potassium conductance, with the numerator increasing faster than the denominator.[9,28,29] As mentioned above, T increases the kinetics of the activation and inactivation gates by a substantial factor. The standard way to quantify temperature dependence is through a Q_{10} factor which quantifies how much a kinetic rate changes upon a 10 °C increase in temperature. For example, the gating kinetics in HH speed up by a factor $\Phi = 3.0^{(T-T_0)/10}$, where T_0 is the reference temperature where the factors are measured. This factor Φ multiples the right hand side of all the gating variable derivatives, thereby increasing their rate of change upon warming, in the same way other chemical reactions are sped up by warming. The Q_{10} factor for the kinetic constants is 3.0 in this example, and in our paper as well. The Q_{10} for the maximal Nav conductance is 1.4,[28,29] while that for Kv is 1.1[28] (see also Table I). These Q_{10}'s are within the physiological range for these respective processes.[20,28–31]

Note that, with respect to the Q_{10} for the pump, we are using the generally accepted model that the rate of an enzymatic reaction varies exponentially with small changes in temperature. In practice, we chose a value of 1.9 for the Q_{10} of the pump that lies between the Q_{10} values for the conductances and the gate kinetics—although we will investigate the effect of this latter value. Our goal was to obtain a generic picture for the effect of T variations on the basic bifurcation diagram of the CLS model. Furthermore, as we will show below, upon sweeping the Q_{pump} at fixed T, there are no surprises: there is a transition from quiescent to bursting. Different values for Q_{pump} will simply shift the bifurcation picture quantitatively.

Note that the precise values for these Q_{10}'s is not so important as dissecting out their individual effects, and more generally, as offering a framework in which to understand the dynamical interactions of T and other parameters. In fact, the results reported below for each T-dependent process can simply be graded along with the magnitude of their associated Q_{10}. We chose 20 °C as the reference temperature to be consistent with previous simulations in Refs. 2, 4, 5, and 24. There is nothing special about this reference temperature. Others could

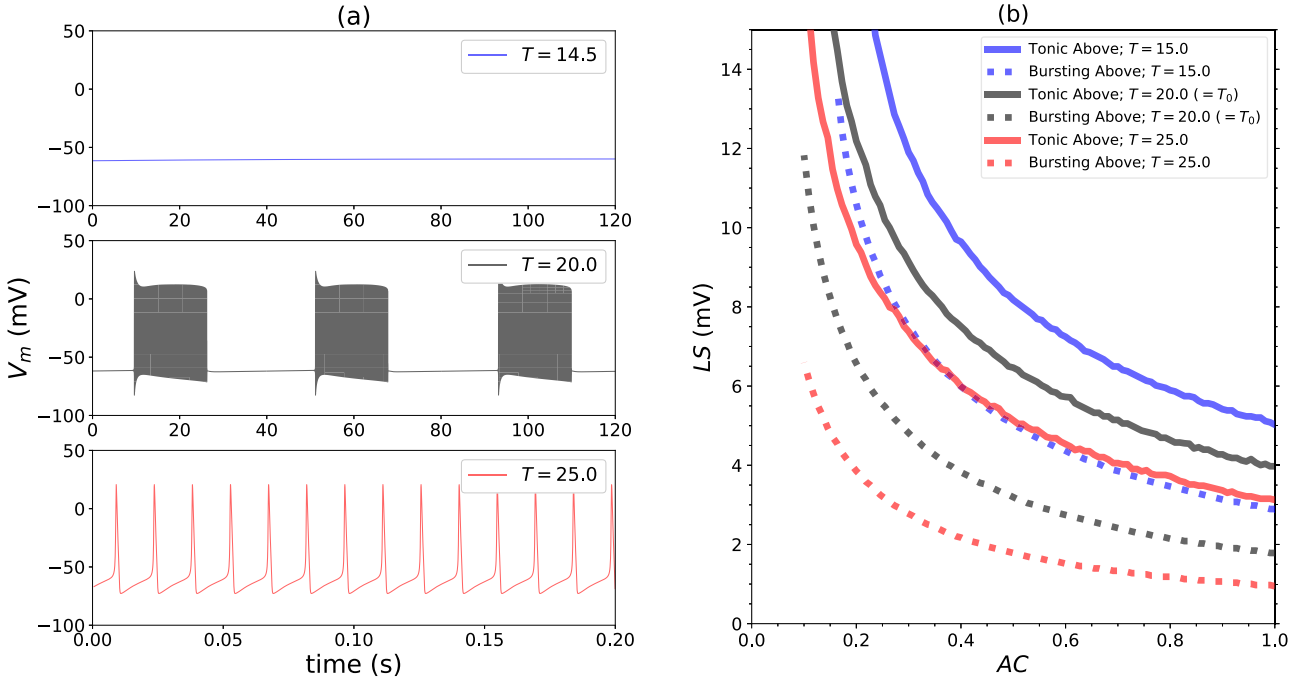

FIG. 2. T-CLS: (a) As *temperature* is varied, the system moves from quiescent, to bursting, to tonic firing; at fixed left-shift (here $LS = 3.0$ mV, $AC = 1$). This effect can be understood in terms of the regime diagram: Temperature moves the ectopic boundary. (b) The dashed and solid lines have the same meaning as in Fig. 1(b). Temperature increases from the top downward.

have been chosen. For example, we could have decided to calibrate our model at 37 °C. Given the dependence of the Nernst potentials on absolute temperature, this simply implies that we would have been working with slightly different ratios of internal to external concentrations. We would expect qualitatively similar results to Fig. 2(b) by increasing/decreasing the temperature by 5 °C.

The Nernst potentials are directly proportional to T as we can see in their definitions above. Their increase with T expresses the fact that the strength of the diffusion of the ions to dissipate their gradients also increases with T. However, for simplicity, the Nernst potential for the weaker leak current, made up mostly of chloride, is given a T-independent value. The same goes for the (weak) maximal leak conductance g_{leak}. The consequences of these choices are highlighted in the Discussion section. Note that the magnitude of the Nernst potentials is directly proportional to temperature, although with temperature being in Kelvins, this is a limited effect for 5°-10° changes. However, their dependence on the effect of T on ionic concentration ratios, due to the pump, is more significant as we will see below.

As mentioned above, there is a more intimate link between our CLS model and cold receptor models on which our temperature analysis is built: both involve bursting oscillations, and their associated subthreshold oscillations (see, e.g., Refs. 20, 21, 26, and 29). However, there are some important dynamical differences. Models of cold receptors burst for a different reason than the CLS model above. They typically possess an endogenous slow-wave oscillation that causes parabolic bursting. The slow wave goes on even if spikes are not present, a clear slow-fast decomposition of the full dynamics. The cold receptor models burst due to a slow subsystem that involves an inward current (such as persistent Na^+) and a slow subthreshold outward current. The latter, although generally thought to involve K^+, has been assigned a more generic mechanism for its activation (see Ref. 26 and references therein), or been given a specific calcium dependence and accompanying calcium buffering dynamics.[20,32] In contrast, leaking Nav channels initiate ectopic firing in the CLS model. This can lead to bursts because the slow dynamics of the Na^+/K^+ pump struggle to restore ion gradients during the active firing phase of ectopic firing. Thus, during the active phase, the Nernst potentials become depleted, and firing stops at some point; the gradients are restored by the pump during this quiescent phase. This CLS burst oscillation does not persist in the absence of firing.

All numerical integrations were carried out using the NEURON simulation environment (www.neuron.yale.edu) running on an Apple laptop computer. The code is based on a Python script stored on ModelDB (http://modeldb.yale.edu/234111).[24] This code allows users to explore the phase diagram in Fig. 1(b) by selecting (AC, LS) coordinates and running simulations. NEURON's built in adaptive time step method (CVode) was used.

III. RESULTS

We will discuss the effect of temperature in terms of the phase diagram of the original coupled left shift (CLS) model. Figure 1(a) shows the behavior observed as the damage is increased at a node with all Nav's left-shifted. The node stays quiescent for small damage up to a critical value, then as LS is increased further the Na^+ current flowing in triggers a burst of APs which lasts for a finite time. In that phase, APs are produced spontaneously until the ion gradients are too depleted to maintain firing with the stimulating I_{Na} current. As LS is

increased further, the interburst time diminishes until comparable to the period of the bursting APs. The system then fires continuously or tonically. The boundaries of the different regions are given in Fig. 1(b). This variant of the Hodgkin-Huxley model (HH) is insensitive to temperature except for small changes to excitability due to the absolute temperature prefactor in the Nernst potentials E_K and E_{Na}.

To study the effect of temperature on CLS-induced spontaneous firing, a set of temperature factors Q_{10}'s are added to the model: Q_{pump}, Q_{Na}, Q_K, and Q_{gate} (values listed in Table I). Figure 2 summarizes the changes to the system's behavior with temperature when these Q_{10}'s are included. In Fig. 2(a), we fix $LS = 3.0\,\text{mV}$ and use temperature to move the system from quiescent, to bursting, to tonic firing. Temperature pushes the system in and out of ectopicity. In Fig. 2(b), we reproduce the ectopic boundaries shown in Fig. 1(b) at three temperatures. At the reference temperature ($T = T_0 = 20.0\,^\circ\text{C}$), the boundaries are unchanged—this is equivalent to the original CLS model. Heating to $T = 25.0\,^\circ\text{C}$ lowers the ectopic boundaries (i.e., spontaneous firing begins with less damage than at the reference temperature). Cooling to $T = 15.0\,^\circ\text{C}$ raises the boundaries—points near the boundary which were ectopic at the reference temperature can be rendered quiescent with moderate cooling. Temperature thus alters the phase diagram by shifting the ectopic boundaries, but qualitatively the story is unchanged.

Heating reinforces left shift, cooling counteracts it. An injured neuron is more sensitive to temperature, and a chilled neuron can remain quiescent at greater left shift. Figure 3 summarizes the combined effect of left-shift and temperature in the form of a new phase diagram, analogous to Fig. 1(b) but in the *T-LS* space. We focused on the first transition (quiescence to bursting) because our objective is to discuss remedial strategies to return an ectopically firing node to quiescence.

Our extended HH model has plenty of moving parts before temperature sensitivity is introduced. To understand the effect of the various Q_{10}'s, we run "knock-in" simulations, wherein a single Q_{10} (e.g., Q_{Na}) is active and the rest are set to unity. These simulations are plotted together in Fig. 4, in which we see that Q_{Na} moves the ectopic boundary significantly more than any of the others. The dominance of Q_{Na} is not surprising: sodium currents determine excitability, and hence ectopicity. Temperature affects every cellular mechanism but its effect on voltage-gated sodium channels dominates here, followed by electrogenic pumps (via Q_{Na} and Q_{pump}, respectively). In Fig. 4(b), we sum the four knock-in simulations' deviations from the reference curve and observe that the result (roughly) reproduces the complete temperature sensitive model.

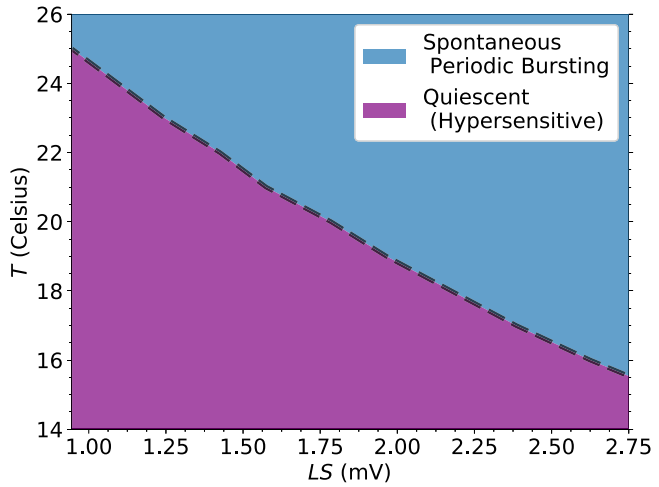

FIG. 3. Another regime diagram: Temperature versus left-shift at $AC = 1$. Temperature and CLS work together—decreasing one allows for an increase in the other. An injured neuron is more sensitive to temperature, and a chilled neuron is more robust to CLS injury [cf. Figs. 1(b) and 2(b)].

To explain the effects of temperature and left shift, we inspect the absolute value of the voltage gated sodium current I_{Na} at V_{rest}. (Taking the absolute value simplifies the discussion. For example, since V_{rest} is negative and E_{Na} is positive, the driving force $(V_{rest} - E_{Na})$ is larger when E_{Na} is strengthened). Writing $\Delta T = T - T_0$, the magnitude of the Nav current is

$$|I_{Na}(V_{rest})| = \overline{g_{Na}} m_\infty^3 h_\infty Q_{Na}^{\Delta T/10}(|V_{rest}| + E_{Na}). \tag{19}$$

Unpacking Eq. (19), from left to right: The activation m and inactivation (availability) h variables are functions of the membrane voltage, but when damaged they respond to V as a healthy one does at $\tilde{V} = V + LS$. In other words, $m = m(V + LS)$ and $h = h(V + LS)$. This means that LS leads to a larger steady state Nav current. The temperature parameter Q_{Na} serves to multiply the entire voltage gated sodium conductance by a factor $Q_{Na}^{\Delta T/10}$, producing a larger current at any given V. T shows up twice in the driving force $|(V - E_{Na})|$. First, the *absolute* temperature multiplies the Nernst potential E_{Na} [see Eq. (17)]. Second, Q_{pump} drives the concentrations $[Na^+]_i$ and $[Na^+]_o$ whose ratio forms the argument of the logarithm in E_{Na}.

The resting potential is not affected by left shift or temperature: Where quiescent solutions exist, the conservation of Na^+ and K^+ ions in our model causes $V_{rest} = E_{leak}$. That is, the resting potential is determined by E_{leak} and therefore is independent of LS and T, as we now show. At $V = V_{rest}$, the current balance equation becomes

$$0 = C\frac{dV}{dt} = -\sum I = -\{I_{Na,total} + I_{K,total} + I_{leak}\}, \tag{20}$$

where each total current includes voltage gated channels, pumps, and leak. The model's explicit ion conservation (via the electrogenic Na^+/K^+ pump) is a helpful constraint. Since at equilibrium each ion's total current is individually zero, Eq. (20) becomes three separate equations:

$$\begin{cases} 0 = I_{Na,total} = [g_{Na} + g_{Na,leak}](V - E_{Na}) + 3I_{pump}, \\ 0 = I_{K,total} = [g_K + g_{K,leak}](V - E_K) - 2I_{pump}, \\ 0 = I_{leak} = g_{leak}(V - E_{leak}). \end{cases} \tag{21}$$

Equation (21) says that to reach equilibrium, the model must tune the sodium and potassium concentrations—using the pump and voltage gated channels—such that $V = E_{leak}$.

The main role of I_{pump} is to restore the Na^+ and K^+ ion gradients. As seen in Eq. (21), equilibrium occurs when the outward (Na^+) and inward (K^+) pump currents are respectively balanced by the conductance and leak currents associated with these ions. The role of the pumps is to maintain ion

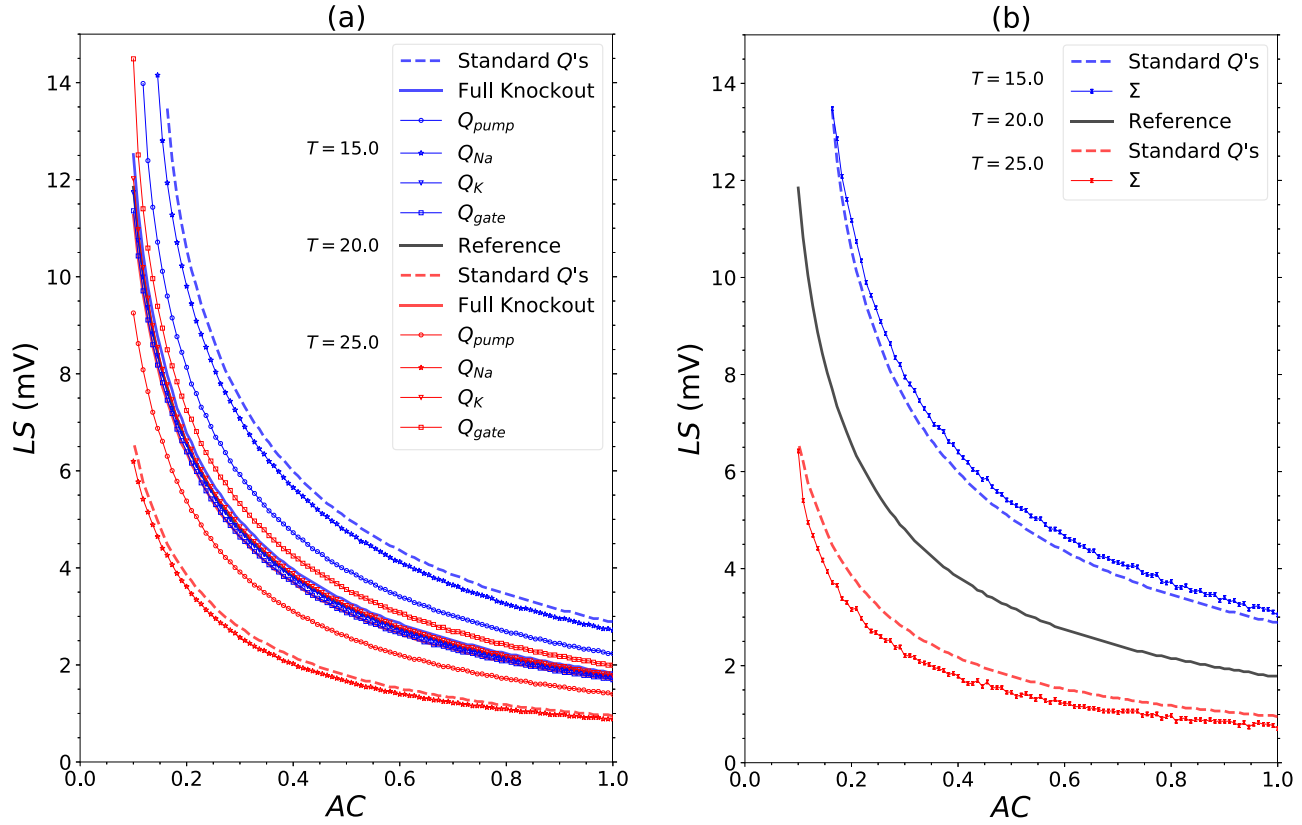

FIG. 4. (a) To isolate the effects of the four Q_{10}'s, Q_{pump}, Q_{Na}, Q_K, and Q_{gate} (listed in Table I), we plot the altered ectopic boundary "one Q_{10} at a time," along with the full knock-out and the reference case of full knock-in. That is, a single Q_{10} is switched on while the rest are set to unity. From this plot, it is clear that Q_{Na} and Q_{pump} dominate temperature's mediation of ectopicity. In (b), the combined effect of the Q_{10}'*s* is roughly recovered by summing the effect of each Q_{10} on its own.

gradients or restore them when depleted by firing. Increased pump currents—following, e.g., an increased Q_{pump} (see Fig. 5 below)—have to be balanced by increased steady-state Na^+ and K^+ currents. Since in our model V_{rest} is set by E_{leak}, which therefore can only change if E_{leak} changes (it is fixed throughout this study), such increased currents can only be achieved with a larger driving force (V-E_X) (where X is either Na^+ or K^+), i.e., an upper shift in the positive E_{Na} and a lowering of the negative E_K. And this is in fact what the pumps accomplish. By pumping out Na^+ and pumping in K^+, the pumps increase the Na^+ and K^+ gradients, leading to larger positive values of E_{Na} and more negative values of E_K. The increase in E_{Na}, notably, increases I_{Na} through the driving force $|(V - E_{Na})|$ [see Eq. (21)]. This has the consequence of lowering the ectopic threshold as T increases even if I_{pump} was the only T-dependent process. In the model with full T-dependence, the increase in the g_{Na} conductance further lowers the ectopic threshold.

The purpose of Fig. 5 is precisely to show this surprising effect of the pumps. In that figure, we show how the different currents behave as the size of the pump current is slowly increased while keeping the operating temperature at $T = 25$ °C and all other Q_{10}'s equal to one for a slightly damaged node ($LS = 1.5$ mV; $AC = 1.0$); this can be interpreted as a ramp in the Q_{pump} value. One sees that the Nernst potentials become bigger in absolute value. Furthermore, at some point, the subthreshold oscillations appear, and eventually a bursting solution occurs, with a very long time interval between active phases, since we are near the bursting/tonic boundary. The presence of the subthreshold oscillations is a consequence that the ramp keeps the transient response alive. In fact, since the linearization of the dynamics around the equilibrium has complex eigenvalues with negative real part prior to burst onset, the ramp expresses the oscillation at a frequency equal to the imaginary component of the eigenvalue. As a whole, the paradox of how a pump that produces a net outflux of positive charge can make the system more excitable is resolved by noting that the concentration ratio $[Na^+]_i/[Na^+]_o$ determines the driving force for the sodium current.

We chose a ramp of Q_{pump} that drives the system across a bifurcation from quiescence to bursting, because the effect of increasing Q_{pump} may be counterintuitive. A hyperbolic tangent ramp was imposed whose asymptotic value is just above the onset of bursting. The bifurcation will occur at different values of Q_{pump} depending on the chosen temperature. In Fig. 5, the temperature is 25 °C.

An analytical demonstration of how cooling moves the quiescent-to-bursting bifurcation boundary to higher values of LS is beyond the scope of our work, but we make a few comments in this direction. Our eight-dimensional dynamical model has a fixed point when the system is quiescent. Effectively, it is only six-dimensional since the total number of Na^+ and K^+ ions is conserved. The voltage component of this fixed point corresponds to the resting potential. Previous bifurcation analyses (see Fig. 2 in Ref. 4) reveal that the fixed point progressively loses stability as LS increases and

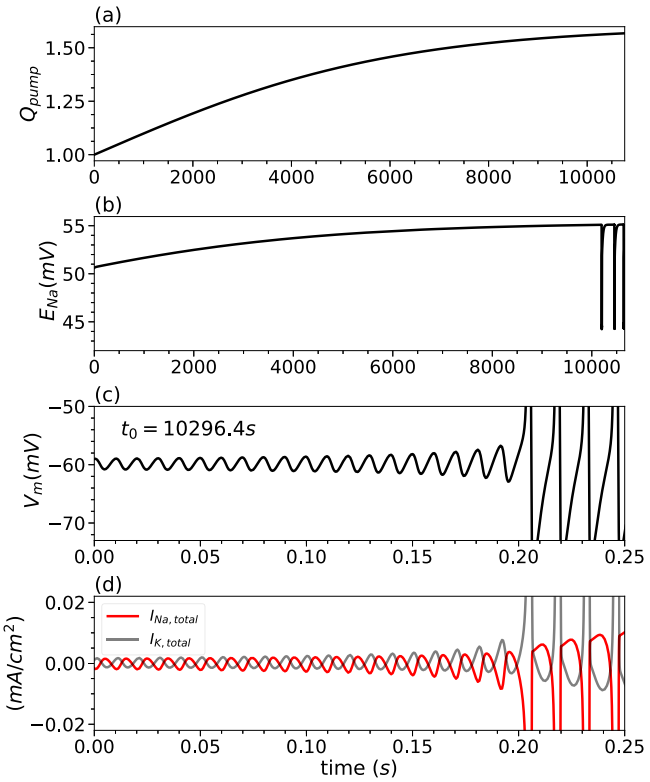

FIG. 5. Response of the system to ramped Q_{pump}, at fixed temperature, and on two time scales. (a) Here Q_{pump} alone is activated (knock in). The initial state is $LS = 1.5$ mV, $AC = 1.0$, and $T = 25$C. Q_{pump} is slowly ramped from a value of 1.0 following a shifted tan$h$ whose $t \to +\infty$ asymptote is slightly above 1.5. (b) Response of E_{Na} during the ramp. The bifurcation to bursting is crossed around 10 000 s when Q_{pump} is about 1.5 [see (a)]. Due to the long timescale, a single spike in E_{Na} here corresponds to an entire burst that lasts about 6 s, and the time duration between bursts is 140 s. The rate during bursting is about 54 Hz. Short timescale: (c) Membrane voltage near the onset of bursting; (d) Total sodium and potassium currents near the onset of bursting.

becomes unstable beyond the quiescent-to-bursting threshold. This results from the increase in the sodium window current at rest. The approach of a bifurcation to sustained firing is a general consequence of increasing the net inward current to an excitable system. Warming also increases the sodium window current through its increase of the pump activity and the conductances, as well as of the Nernst potentials, both directly and via the higher concentration gradients caused by a stronger pump [see Fig. 5(b)]. This increased sodium ion current overrides the opposing effect of the increased kinetic rates [Fig. 4(a)], and further destabilizes the fixed point for a given *LS*; cooling stabilizes this point and can thus undo some of the effect of *LS*.

Finally to test the robustness of the effects of cooling, additive (current) noise on the current balance equation was included and integrated using the Euler-Maruyama algorithm (not shown). The cooled node which was shown in Fig. 2(a) remains quiescent with subthreshold oscillations driven by the noise, and very rare spiking. When the system is brought closer to threshold, the noise induces bursts of varying duration, as in Yu *et al.*[4] Thus, a preliminary analysis of the effect of current noise on T-CLS suggests that it modifies the dynamics as in the CLS case.

IV. DISCUSSION

We have considered the dynamics of the standard HH equations with two concomitant parameter changes: (1) the midpoint voltage for Nav activation and inactivation, duly shifted to a lower (more negative) value due to a CLS phenomenon; and (2) temperature changes. Of the two, the former is clearly the more delicate one from a dynamical point of view, as it enables the cell to start firing in the absence of any input. Specifically, the pumps cannot keep up their ionic balancing act in the presence of enhanced Na^+ leakiness, and the Nernst potentials start to collapse during sustained firing, such that the behavior that appears after quiescence in a mildly injured cell is bursting. The bifurcations underlying the successive transition between quiescence, bursting, and tonic as the left shift increases have been worked out in much detail.[4]

Interestingly, temperature does not change this state of affairs qualitatively, but rather only quantitatively for the range of parameters we have explored. In other words, changing the maximal conductances and the kinetic rates for the gates and the pumps still leads to a picture where quiescence goes to bursting and then tonic, albeit at higher *LS* values when T is lowered. In some as of yet unexplored part of parameter space, temperature changes may have a more drastic effect on the bifurcations leading to bursting and tonic limit cycle solutions. Regardless, the fact that the thresholds are simply moved around by temperature is potentially attractive from an intervention point of view: one can expect a fairly straightforward effect of cooling on a traumatized nerve.

In the absence of any Q_{10}'s, the sole temperature dependence of our model stems from the direct proportionality of the Nernst potentials to absolute temperature. As we saw in Fig. 4, this modifies the boundary for ectopic behavior only very slightly, but in the same direction: cooling raises the threshold, while warming lowers it. By allowing only one temperature dependency to take effect at once, we found [Fig. 4(a)] that the sodium current I_{Na} is the main player in moving the boundary; the Na^+/K^+ pump comes in second, contributing a threshold shift of about a third of that of Q_{Na}. In contrast, the effect of K^+ is rather minimal, although in the opposite direction; this is not surprising since it has the smallest Q_{10}. Interestingly, only the gating kinetics have a significant effect that is opposite to that of all the other factors considered here [Fig. 4(a)].

Our knock-in simulations also reveal that, to a good approximation, the total effect of temperature on the quiescent-bursting boundary is given by the algebraic sum of these effects [Fig. 4(b)]. We have also done single knock-out simulations, where only one Q_{10} at a time (for the pump, Nav, Kv, or the gates) is set equal to 1. Those results support the conclusions from the knock-in and summing simulations, and for that reason are not shown.

The effect of T lies in the fact that the total Nav current is made up of an *LS*-dependent but T-independent gating factor (m^3h), multiplied by a *LS*-independent but T-dependent battery term. It is also interesting that the resting potential is insensitive to the value of *LS* or of T. In fact, by construction, V_{rest} is always equal to E_{leak} in our model. Here is the result

of our more detailed formulation of HH dynamics that tallies every Na^+ or K^+ ion going across the membrane and that includes the Na^+/K^+ exchanger by necessity. In fact, the ionic species' currents are individually balanced and sum to zero in the resting state, i.e., the quiescent state where no firings occur. This is necessary to avoid continual accumulation of an ionic species on one side of the membrane or the other. Hence in the resting state, the total Na^+ and K^+ currents are individually zero; from the current balance equation, this implies that $V_{rest} = E_{leak}$.

This value contrasts with the well-known standard HH system, which has four state variables (voltage, Nav activation and inactivation gates, and Kv activation date). In that system, V_{rest} is not necessarily E_{leak}, but rather the root of a more complex set of nonlinear equations involving all the conductances and the Nernst potentials. In the standard HH, V_{rest} depends on T and LS, even though experimentally the resting potential in squid axon does not depend significantly on T.

Relatedly, we have assumed that the mechanisms meant to keep the chloride gradient across the membrane constant are affected minimally by the mild injury. This means that the Nernst potential for chloride is unaffected by the mild injury. However, like all Nernst potentials, the magnitude of E_{leak} will be proportional to absolute T. Furthermore, it is reasonable to assume that the maximal leak conductance g_{leak}, as well as the smaller Na^+ and K^+ leakages through the pump, will have a Q_{10}. For the pump leakage, this effect is likely quite small. As for g_{leak}, it may have a Q_{10} on the order of the ones given the Na^+ and K^+ conductances. But the leak conductance is often an order of magnitude less than those of the fast spiking Nav and Kv conductances, and the battery term is small near resting potential. Incorporating these extra T-dependencies may amount to an increased stabilization of the quiescent state as T increases, since V_{rest} should decrease slightly following the increase with T due to both factors entering I_{leak} (i.e., the conductance and the battery term). It is to be seen how this plays out in a given experimental system, with its own complement of ions making up the leakage currents and their associated temperature dependencies. But at the very least, it would seem that making the leak terms thermosensitive could "offset the offset" a bit, i.e., offset the potential benefit of cooling for reversing mild traumatic injury.

Our work has focused on a single node of Ranvier and found that the ectopy brought upon by CLS can be counteracted by cooling. While the results were obtained in the specific context of a node, the fact that the model revolves around an expanded HH system with plausible Q_{10} values suggests that it is generically applicable to any system where this model provides a good description of the un-traumatized dynamics at ordinary temperatures.

While our study suggests that cooling can alleviate the symptoms of CLS and its associated neuropathic pain, it also predicts that warming will exacerbate the injury by lowering the threshold for ectopic activity. In the pain literature, allodynia describes the situation where a normally non-painful mild stimulus (mechanical, temperature, etc.) becomes painful. In this sense, the heightened ectopic activity in our model brought on by warming could partly underlie "hot allodynia" seen clinically. It is not clear how large temperature changes can be in the context of our CLS model, the experimental basis for which was determined at a fixed reference temperature. This argues for a better calibration of the temperature between model and CLS experiments to begin making quantitative predictions, and also for doing CLS experiments at different temperatures to see if the coupled-left shift is always the right picture, at least for sodium.

One has to recognize that this is a simplified yet necessary preliminary step toward understanding the effects of temperature on normal and injured or diseased states. There are many factors at play, and our model captures a small number of them. For example, a recent study[33] reported that cooling induced undesirable changes in motor axons that were consistent with depolarization; yet, the effect on sensory axons was comparatively deemed "more complicated" as it may involve different expression levels of hyperpolarization-activated channels. And, there are many different parameter changes that can be investigated in detailed model systems such as Aplysia, beyond the simple generic ones considered here.[34] A further consideration is the modeling of the electrogenic pump. Classic work has shown that the membrane potential in squid axon is T-independent; our model reproduces that finding. However, this property varies across neurons; for example, membrane potential increases with warming in mammalian optic nerve,[35] a property ascribed to a combination of the electrogenic pump modeled here as well as other electrically neutral mechanisms of sodium entry. Clearly, a specific model system in which many effects can be studied is a valuable tool, and generalizations must be done with caution.

We note that current state-of-the-art models of thermoreception actually avoid the question of the Q_{10} for the pump by omitting the pump altogether.[27,31] Willis *et al.*[25] and Wiederhold and Carpenter[26] have paid special attention to the Na^+/K^+ electrogenic pump, stating that its activity increases with temperature, and since its net effect is hyperpolarizing, temperature increases should hyperpolarize the membrane potential. This effect is incorporated in our model, given that every cycle of the pump produces a net outflux of positive charge. Curiously, increasing temperature when only the Na^+/K^+ pump is assumed to be T-dependent [i.e., knocked-in: see Fig. 4(a)] leads to a lowering of the threshold, meaning that effectively the system is depolarized. The reason why this occurs is due to an indirect effect on the Nernst potential for Na^+: increased pump activity makes E_{Na} more positive, due to the increased disparity between inner and outer Na^+ concentrations. Given that the battery term (V-E_{Na}) is a main component of I_{Na}, the net effect of increased pump activity is a depolarization. The magnitude of this effect will of course depend on the precise value of Q_{pump}, which in our study was intermediate between that of the maximal conductances (1.1 and 1.4) and of the gate kinetics (3).

Future work will consider the propagation aspects of the proposal put forth here, as was done for the CLS effect.[5] In particular, while CLS may be confined to a certain area of the nerve, it may be challenging to alter the temperature only at these areas. One may then contend with the desired effect in the traumatized area, along with potentially undesirable effects nearby where a healthy nerve is cooled,

which would impede its normal excitability. Ultimately, the precise beneficial effects of temperature, if any, will depend on how well the CLS model captures the mild traumatic injury in the first place, and whether the injury is indeed mild or not. Other temperature-dependent processes may also be at play. And there are specific forms of neuropathic pain that involve temperature sensation, such as cold allodynia. It remains to be seen whether the model described here is relevant to that specific condition. Another factor is that transients may play a role, since it is known that the effect of CLS can become "expressed" only once a neuron tries to propagate action potentials.[5] Thus, there may be interesting neural use-dependent effects that one could try to mitigate with temperature. The results presented here suggest that cooling should also mitigate this kind of stimulus-induced ectopicity.

ACKNOWLEDGMENTS

This work was supported by the Natural Sciences and Engineering Research Council (Canada).

[1]J. A. Wang, W. Lin, T. Morris, U. Banderali, P. F. Juranka, and C. E. Morris, "Membrane trauma and Na+ leak from Nav1.6 channels," Am. J. Physiol. **297**, C823–C834 (2009).
[2]P. A. Boucher, B. Joós, and C. E. Morris, "Coupled left-shift of Nav channels: Modeling Na^+ loading and dysfunctional excitability of damaged axons," J. Comput. Neurosci. **33**, 301–319 (2012).
[3]A. L. Hodgkin and A. F. Huxley, "A quantitative description of membrane current and its application to conduction and excitation in nerve," J. Physiol. **117**, 500–544 (1952).
[4]N. Yu, C. E. Morris, B. Joos, and A. Longtin, "Spontaneous excitation patterns computed for myelinated axons with injury-like impairments of nodal Na/K pumps and sodium channels," PLoS Comput. Biol. **8**(9), e1002664 (2012).
[5]M. Lachance, A. Longtin, C. E. Morris, N. Yu, and B. Joos, "Leak/pump dynamics in a model of mild axonal injury yield neuropathic input/output abnormalities in saltatory propagation," J. Comput. Neurosci. **37**, 523–531 (2014).
[6]R. Amir, M. Michaelis, and M. Devor, "Membrane potential oscillations in dorsal root ganglion neurons: Role in normal electrogenesis and neuropathic pain," J. Neurosci. **19**, 8589 (1999).
[7]Y. Kovalsky, R. Amir, and M. Devor, "Simulation in sensory neurons reveals a key role for delayed Na current in subthreshold oscillations and ectopic discharge: Implications for neuropathic pain," J. Neurophysiol. **102**, 1430–1442 (2009).
[8]J. S. Choi and S. G. Waxman, "Physiological interactions between Na(v)1.7 and Na(v)1.8 sodium channels: A computer simulation study," J. Neurophysiol. **106**, 3173–3184 (2011).
[9]D. O. Carpenter, "Ionic and metabolic bases of neuronal thermosensitivity," Fed. Proc. **40**, 2808–2813 (1981).
[10]H. Franssen, G. H. Wieneke, and J. H. J. Wokke, "The influence of temperature on conduction block," Muscle Nerve **22**, 166–173 (1999).
[11]C. Tai, J. Wang, J. R. Roppolo, and W. C. de Groat, "Relationship between temperature and stimulation frequency in conduction block of amphibian myelinated axon," J. Comput. Neurosci. **26**, 331–338 (2009).
[12]G. J. M. Rutten, R. D. A. Gaasbeek, and H. Franssen, "Decrease in nerve temperature: A model for increased temporal dispersion," Electroencephalogr. Clin. Neurophysiol. **109**, 15–23 (1998).
[13]M. Rasminsky, "The effects of temperature on conduction in demyelinated single nerve fibers," Arch. Neurol. **28**, 287–292 (1973).
[14]K. J. Smith, "Conduction properties of central demyelinated and remyelinated axons, and their relation to symptom production in demyelinating disorders," Eye **8**, 224–237 (1994).
[15]H. A. Choi, N. Badjatia, and S. A. Mayer, "Hypothermia for acute brain injury—Mechanisms and practical aspects," Nat. Rev. Neurol. **8**, 214–222 (2012).
[16]M. C. Kiernan, K. Cikurel, and H. Bostock, "Effects of temperature on the excitability properties of human motor axons," Brain **124**(Pt 4), 816–825 (2001).
[17]H. Bade, H. A. Braun, and H. Hensel, "Parameters of the static burst discharge of lingual cold receptors in the cat," Pfluegers Arch. **382**, 1–5 (1979).
[18]H. A. Braun, H. Bade, and H. Hensel, "Static and dynamic discharge patterns of bursting cold fibers related to hypothetical receptor mechanisms," Pfluegers Arch. **386**, 1–9 (1980).
[19]H. A. Braun, K. Schäfer, H. Wissing, and H. Hensel, "Periodic transduction processes in thermosensitive receptors," in *Sensory Receptor Mechanisms*, edited by W. Hamann and A. Iggo (World Scientific, Singapore, 1984), pp. 147–156.
[20]A. Longtin and K. Hinzer, "Encoding with bursting, subthreshold oscillations and noise in mammalian cold receptors," Neural Comput. **8**, 215–255 (1996).
[21]H. A. Braun, M. T. Huber, M. Dewald, K. Schäfer, and K. Voigt, "Computer simulations of neuronal signal transduction: The role of nonlinear dynamics and noise," Int. J. Bifurc. Chaos **8**, 881–889 (1998).
[22]W. L. Maxwell, "Histopathological changes at central nodes of Ranvier after stretch injury," Microsc. Res. Tech. **34**, 522–535 (1996).
[23]A. Ochab-Marcinek, G. Schmid, I. Goychuk, and P. Hänggi, "Noise-assisted spike propagation in myelinated neurons," Phys. Rev. E **79**, 011904 (2009).
[24]B. Joos, B. M. Barlow, and C. E. Morris, "Calculating the consequences of left-shifted Nav channel activity in sick excitable cells," in *Voltage-Gated Sodium Channels: Structure, Function and Channelopathies. Handbook of Experimental Pharmacology*, edited by M. Chahine (Springer, Cham), Vol. 246.
[25]J. A. Willis, G. L. Gaubatz, and D. O. Carpenter, "The role of the electrogenic sodium pump in modulation of pacemaker discharge of Aplysia neurons," J. Cell. Physiol. **84**, 463–471 (1974).
[26]M. L. Wiederhold and D. O. Carpenter, in *Cellular Pacemakers, Vol. 2: Function in Normal and Diseased States*, edited by D. O. Carpenter (Wiley-Interscience, New York, 1982), pp. 27–58.
[27]E. Olivares, S. Salgado, J. P. Maidana, G. Herrera, M. Campos, R. Madrid, and P. Orio, "TRPM8-dependent dynamic response in a mathematical model of cold thermoreceptor," PLoS One **10**(10), e0139314 (2015).
[28]A. L. Hodgkin and R. D. Keynes, "Active transport of cations in giant axons from Sepia and Loligo," J. Physiol. **128**, 2840 (1955).
[29]J. R. Schwarz, "The effect of temperature on Na currents in rat myelinated nerve fibres," Pflugers Arch. **406**, 397 (1986).
[30]B. Hille, *Ionic Channels of Excitable Membranes*, 2nd ed. (Sinauer, Sunderland, MA, 1992); 3rd ed. (2001); for Q10 values, see p. 51.
[31]M. T. Huber and H. A. Braun, "Stimulus-response curves of a neuronal model for noisy subthreshold oscillations and related spike generation," Phys. Rev. E **73**, 041929 (2006).
[32]K. Schäfer, H. A. Braun, and H. Hensel, "Static and dynamic activity of cold receptors at various calcium levels," J. Neurophysiol. **47**, 1017–1028 (1982).
[33]M. O. Kovalchuk, H. Franssen, L. J. Van Schelven, and B. T. H. M. Sleutjes, "Comparing excitability at 37°C versus at 20°C differences between motor and sensory axons," Muscle Nerve **57**, 574–580 (2018).
[34]N. G. Hyun, K. H. Hyun, K. Lee, and B. K. Kaang, "Temperature dependence of action potential parameters in Aplysia neurons," Neurosignals **20**, 252–264 (2012).
[35]T. A. Coates, O. Woolnough, J. M. Masters, G. Asadova, C. Chandrakumar, and M. D. Baker, "Acute temperature sensitivity in optic nerve axons explained by an electrogenic membrane potential," Pflugers Arch. **467**, 2337–2349 (2015).